LM-07K005
February 12, 2007

Computing the External Magnetic Scalar Potential due to an Unbalanced Six-Pole Permanent Magnet Motor

J Selvaggi, S Salon, O Kwon, MVK Chari

Computing the External Magnetic Scalar Potential due to an Unbalanced Six-Pole Permanent-Magnet Motor

Dr. J. Selvaggi, Dr. S. Salon, Dr. O. Kwon, and Dr. M.V.K. Chari
Electrical, Computer, and Systems Engineering Department
Rensselaer Polytechnic Institute in Troy, NY

Abstract

The accurate computation of the external magnetic field from a permanent magnet motor is accomplished by first computing its magnetic scalar potential. In order to find a solution which is valid for any arbitrary point external to the motor, a number of proven methods have been employed. Firstly, A finite element model is developed which helps generate magnetic scalar potential values valid for points close to and outside the motor. Secondly, charge simulation is employed which generates an equivalent magnetic charge matrix. Finally, an equivalent multipole expansion is developed through the application of a toroidal harmonic expansion. This expansion yields the harmonic components of the external magnetic scalar potential which can be used to compute the magnetic field at any point outside the motor.

INTRODUCTION

In order to accurately compute the external magnetic field from a permanent-magnet motor valid for both the near-field and the far-field, a technique which employs toroidal harmonics is developed. This method is most useful for validating magnetic field measurements close to the hull of a cylindrical motor and for accurately predicting the far-field solution when other methods, such as a finite element analysis, are not very accurate.

The well-known method of *charge simulation*, nicely explained in Schwab (1988), is employed so that the permanent magnet motor may be replaced by its equivalent charge distribution on an external circular cylinder. This technique was first employed by Kwon *et al.* (2004) for studying the external field from a permanent magnet motor. Kwon implemented this method for a spherical system. However, in order to more accurately map the geometry of a motor, a circular cylindrical geometry is more useful.

FORMULATION

Charge simulation and the magnetic scalar potential

Schwab (1988) describes charge simulation, as it is applied to an electrostatic system, quite succinctly. He states that: "In the charge-simulation method a configuration of simulation charges is determined whose potential function $\Phi_s(\mathbf{r})$ approximates the true potential function of a physical electrode connected to a voltage source(electrode potential Φ_E). In order to find the required configuration, n unknown point charges $q_1 ... q_n$ are positioned inside the electrode, their positions being defined by the user,..." One can generalize this technique to tackle magnetic systems. In other words, one can rewrite Schwab's definition as follows: charge simulation is a general method by which a configuration of simulation charges is determined, and whose potential function or field function approximates the true potential or field of the actual electric or magnetic source. The first type of charge simulation, used in this paper, is that derived from a known magnetic scalar potential function. The second type of charge simulation, illustrated in Selvaggi (2005), is that derived from experimental data such as the normal component of the magnetic flux density measured on a closed hypothetical cylinder surrounding a real magnetic source.

Using a technique introduced by Kwon *et al.* (2004) for spherical geometries, a magnetic scalar potential column vector is computed on a hypothetical cylindrical grid which encloses the permanent-magnet motor. The potential vector is then used to compute a fictitious magnetic charge matrix by using charge simulation. Figures 1 and 2 illustrate the method.

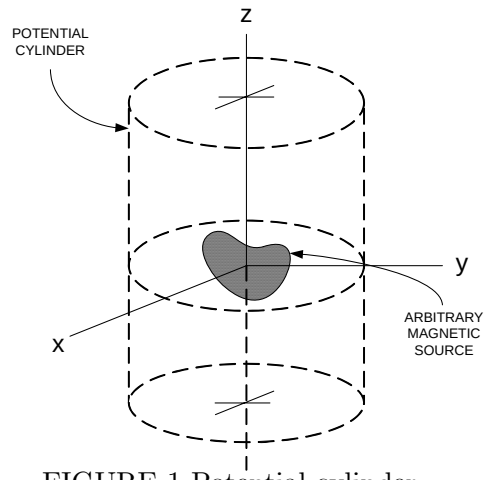

FIGURE 1 Potential cylinder

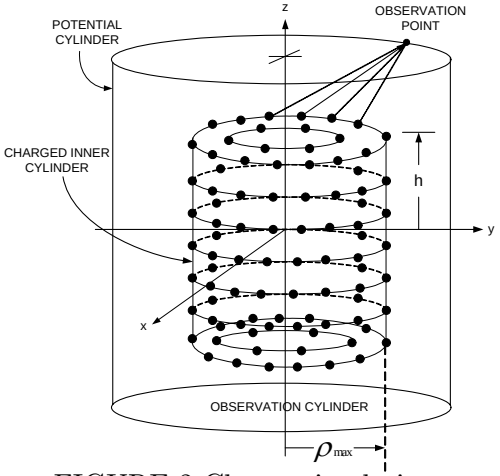

FIGURE 2 Charge simulation

The hypothetical cylinder surrounding any arbitrary magnetic source, shown in Figure 1, will be designated as the *potential cylinder*. The basic idea of charge simulation for a magnetic system is to replace the actual magnetic source with a new source made up entirely of fictitious magnetic charges which yields the same computed potentials on the potential cylinder as the original source did. This is shown in Figure 2. The *charge cylinder* completely encloses the actual source, but lies inside the potential cylinder.

Once the charge cylinder is found which reproduces the correct potentials on the potential cylinder, one can use the charge cylinder and the magnetic form of Coulomb's law (Stratton 1941) to compute the magnetic scalar potential or the magnetic field anywhere external to this new source. In contrast to finite-difference and finite-element methods, the charge simulation method is well suited for unbounded electromagnetic problems, but can be modified to handle bounded problems. The hypothetical surface used in charge simulation could be any closed surface surrounding the real source. However, choosing the appropriate geometry that fits the particular problem may simplify the analysis. The circular cylindrical coordinate system is most suited to real motor geometries.

The mathematical steps employed in charge simulation are given by Equations (1) and (2). Equation (1) is simply the matrix-form of Coulomb's law. The column vector given on the left-hand side of Equation (1) represents the computed magnetic scalar potentials, $[\Phi]$. The square matrix shown on the right-hand side of Equation (1) represents the *inverse distance matrix* where r_{ij} is the distance between the source point and the observation point.

$$\begin{bmatrix} \Phi_1 \\ \\ \Phi_2 \\ \vdots \\ \\ \Phi_n \end{bmatrix} = \frac{1}{4\pi} \begin{bmatrix} \frac{1}{r_{11}} & \frac{1}{r_{12}} & \cdots & \frac{1}{r_{1n}} \\ \\ \frac{1}{r_{21}} & \frac{1}{r_{22}} & \cdots & \frac{1}{r_{2n}} \\ \vdots & \vdots & \ddots & \vdots \\ \\ \frac{1}{r_{n1}} & \frac{1}{r_{n2}} & \cdots & \frac{1}{r_{nn}} \\ \\ \end{bmatrix} \begin{bmatrix} \Omega_1 \\ \\ \Omega_2 \\ \\ \vdots \\ \\ \Omega_n \end{bmatrix} \tag{1}$$

In order to compute the fictitious magnetic charge column vector, $[\Omega]$, one needs to compute the inverse of the $\left[\frac{1}{r_{ij}}\right]$ matrix as shown in Equation (2).

$$\begin{bmatrix} \Omega_1 \\ \\ \Omega_2 \\ \vdots \\ \\ \Omega_n \end{bmatrix} = 4\pi \begin{bmatrix} \frac{1}{r_{11}} & \frac{1}{r_{12}} & \cdots & \frac{1}{r_{1n}} \\ \\ \frac{1}{r_{21}} & \frac{1}{r_{22}} & \cdots & \frac{1}{r_{2n}} \\ \vdots & \vdots & \ddots & \vdots \\ \\ \frac{1}{r_{n1}} & \frac{1}{r_{n2}} & \cdots & \frac{1}{r_{nn}} \\ \\ \end{bmatrix}^{-1} \begin{bmatrix} \Phi_1 \\ \\ \Phi_2 \\ \\ \vdots \\ \\ \Phi_n \end{bmatrix} \tag{2}$$

Once the $[\Omega]$ vector is computed, one can expand the potential of a unit point charge in terms of the free-space Green's function expansion given by Jackson (1999), Smythe (1968), and Bouwkamp and Bruijn (1947). In cylindrical coordinates, the free-space Green's function leads to an expression for the inverse distance between the source point and the field point as shown in Figure 3.

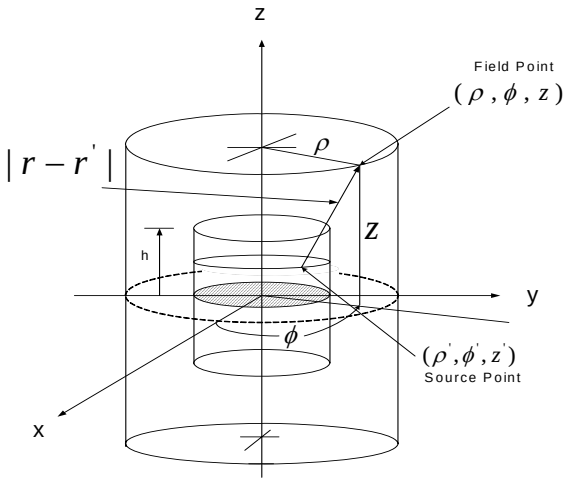

FIGURE 3 The circular cylindrical model

The inverse distance is given by

$$\frac{1}{|\mathbf{r}-\mathbf{r}'|} = \frac{1}{\sqrt{\rho^2 + a^2 + z^2 - 2a\rho\cos(\phi - \phi')}}. \tag{3}$$

This relation for the inverse distance can be written in terms of a Fourier series expansion whose weighting coefficients are the Legendre functions of the second kind and of half-integral degree (Lebedev 1965). These are also called toroidal functions of zeroth order or Q-functions (Snow 1949, 1952) and (Hobson 1900). The expansion is given by

$$\frac{1}{|\mathbf{r}-\mathbf{r}'|} = \frac{1}{\pi\sqrt{\rho\rho'}} \sum_{m=0}^{\infty} \epsilon_m Q_{m-\frac{1}{2}}(\xi) \cos\left[m\left(\phi - \phi'\right)\right], \tag{4}$$

Equation (4) can be viewed as a Fourier series expansion of the inverse distance function whose weighting coefficients are Q-functions. This expansion is also a toroidal harmonic expansion where $\xi = \frac{\rho^2 + \rho'^2 + (z-z')^2}{2\rho\rho'} > 1$. The Neumann factor (Morse and Feshbach 1953), ϵ_m is 1 for $m = 0$, and 2 for all $m \geq 1$. It is shown in Selvaggi *et al.* (2004) that

$$Q_{m-\frac{1}{2}}(\xi) = \frac{\pi}{(2\beta_k)^{m+\frac{1}{2}}\, 2^m} \sum_{n=0}^{\infty} \frac{(4n+2m-1)!!}{2^{2n}\,(n+m)!n!} \frac{1}{(2\xi)^{2n}}. \tag{5}$$

When a magnetic field is produced from an arbitrary source, the application of charge simulation along with the magnetic form of Coulomb's law will allow one to compute the magnetic field external to an equivalent cylindrical source. The matrix form of Coulomb's law for hypothetical magnetic charges can be written in summation-form as

$$\Phi_P(\rho, \phi, z) = \frac{1}{4\pi} \sum_{k=1}^{N} \frac{\Omega_k}{|\mathbf{r} - \mathbf{r}_k|}, \tag{6}$$

where $\Omega_k(ampers \cdot meters)$ are the hypothetical magnetic charges. The units for magnetic scalar potential are in *amperes*.

From (4), (5), and (6), one can compute the corresponding magnetic scalar potential at some observation point given in cylindrical coordinates. This is written as

$$\Phi_P(\rho,\phi,z) = \frac{1}{4\pi^2}\sum_{k=1}^{N}\frac{\Omega_k}{\sqrt{\rho\rho_k}}\sum_{m=0}^{\infty}\epsilon_m Q_{m-\frac{1}{2}}(\xi_k)\cos\left[m(\phi-\phi_k)\right], \tag{7}$$

where $\xi_k = \frac{\rho^2+\rho_k^2+(z-z_k)^2}{2\rho\rho_k} > 1$. The magnetic field intensity at any point in space external to the charged cylinder can be found from

$$\mathbf{H} = -\boldsymbol{\nabla}\Phi_P(\rho,\phi,z), \tag{8}$$

where the gradient is taken in cylindrical coordinates.

REAL 6 POLE MOTOR

A real $6-pole$ permanent-magnet brushless DC motor including permanent magnets, stator iron, winding currents, and endcaps is used to test the toroidal expansion. Figure 4 shows the finite element model of the $6-pole$ motor. Details are found in Kwon's thesis (2004).

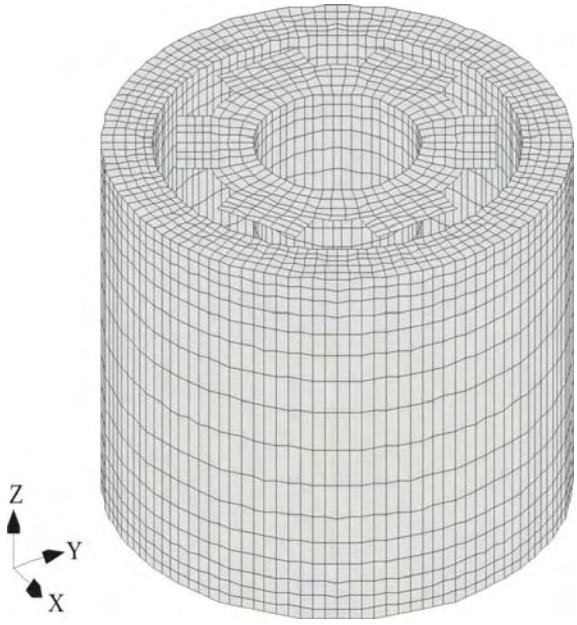

FIGURE 4 Finite element model of 6-pole motor

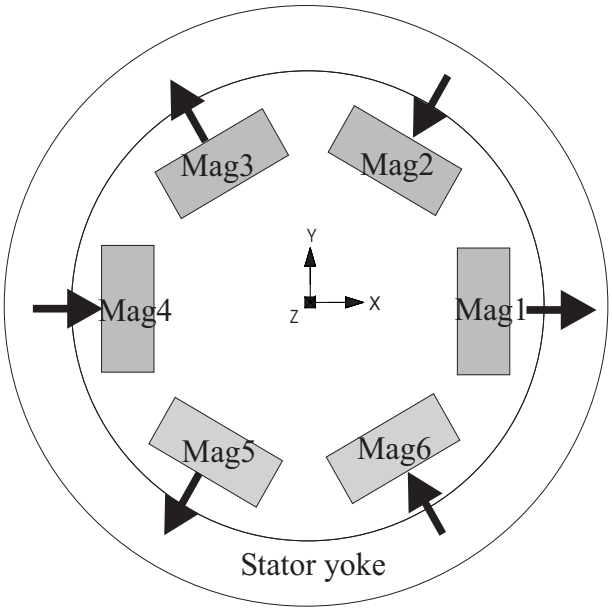

FIGURE 5 Permanent magnet pole arrangement

Figure 5 represents the pole arrangement of the $6-pole$ motor. Employing Equations (2) and (7), one is able to compute the magnetic scalar potential from a real permanent magnet motor. Two basic models can be considered. The first assumes that the motor is perfectly balanced and the second considers various asymmetries that may exist because of manufacturing tolerances, defects, etc.

Balanced motor

The plot of the total scalar potential for a balanced $6-pole$ motor is shown in Figure 6

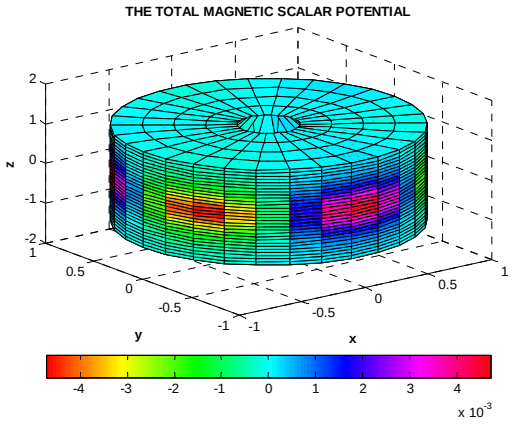

FIGURE 6 This is the total $\Phi_P(\rho, \phi, z)$

Figures 7 through 11 represent the various components which contribute to the magnetic scalar potential of a real $6-pole$ motor under full load conditions.

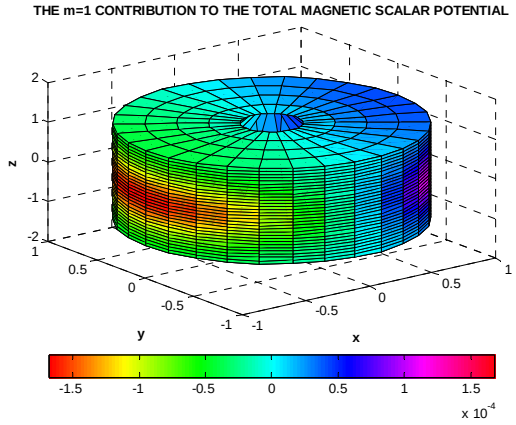

FIGURE 7 This is the $\Phi_P^{(1)}(\rho,\phi,z)$ component

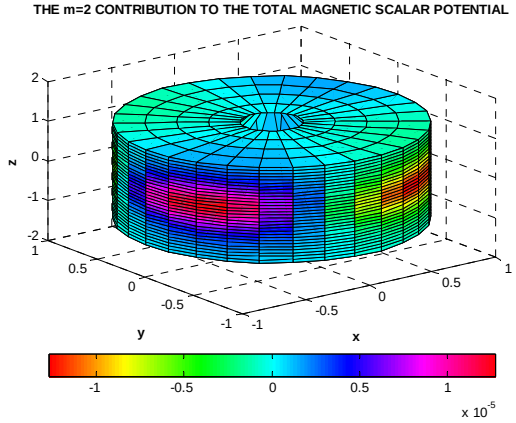

FIGURE 8 This is the $\Phi_P^{(2)}(\rho,\phi,z)$ component

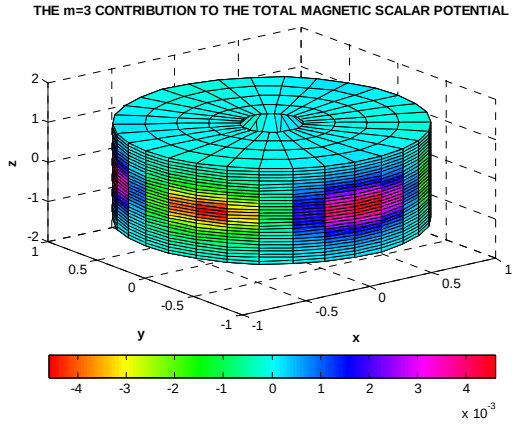

FIGURE 9 This is the $\Phi_P^{(3)}(\rho,\phi,z)$ component

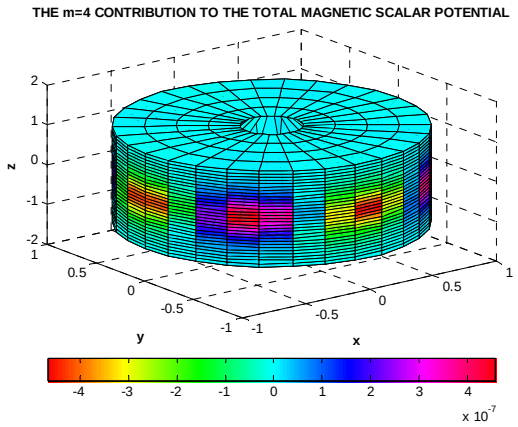

FIGURE 10 This is the $\Phi_P^{(4)}(\rho, \phi, z)$ component

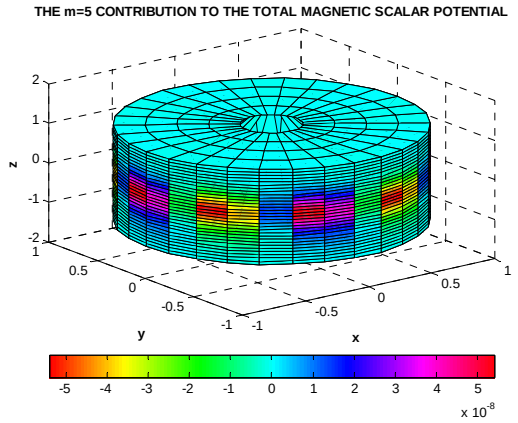

FIGURE 11 This is the $\Phi_P^{(5)}(\rho, \phi, z)$ component

Unbalanced motor

The plot of the total scalar potential for an unbalanced $6-pole$ motor with a 6.5 % demagnetization of magnet number 4 is illustrated in Figure 12.

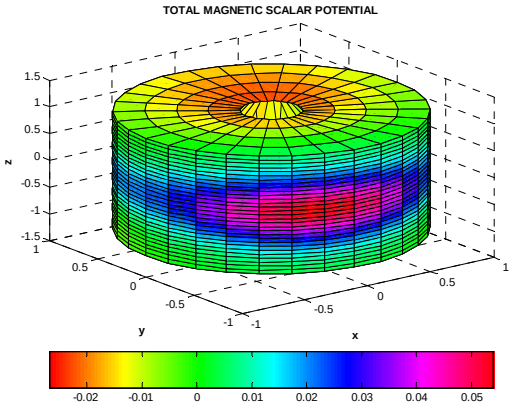

FIGURE 12 This is the total $\Phi_P(\rho, \phi, z)$

Figures 13 through 15 represent the various components which contribute to the magnetic scalar potential of the unbalanced motor.

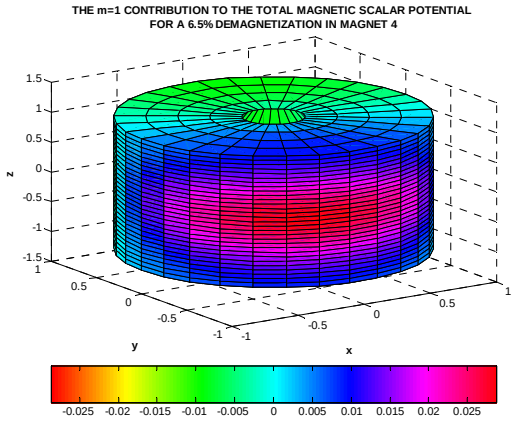

FIGURE 13 This is the $\Phi_P^{(1)}(\rho, \phi, z)$ component

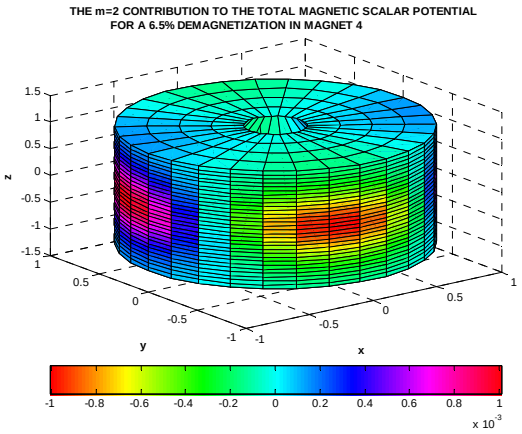

FIGURE 14 This is the $\Phi_P^{(2)}(\rho, \phi, z)$ component

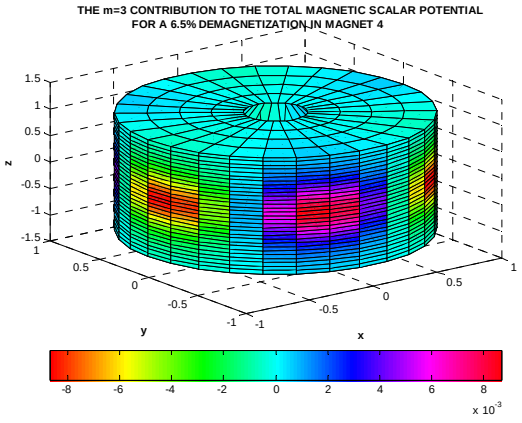

FIGURE 15 This is the $\Phi_P^{(3)}(\rho, \phi, z)$ component

This analysis yields a simple illustration of how a demagnetized magnet can interrupt the symmetry that is associated with the balanced motor considered previously.

Consider the case where only a fairly large axial off-set exists. Figures 16 is a plot of the total magnetic scalar potential when for the $6-pole$ motor with a 10 % axial off-set.

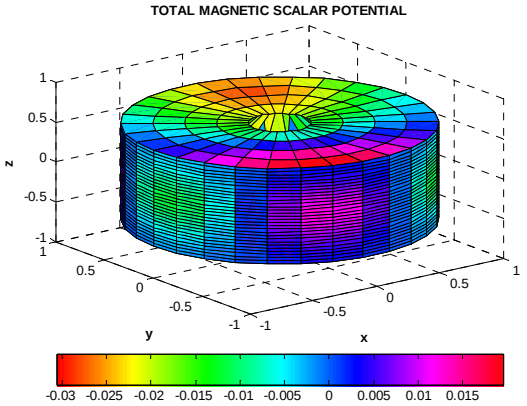

FIGURE 16 This is the total $\Phi_P(\rho,\phi,z)$

Figures 17 through 19 represent the various components which contribute to the magnetic scalar potential of the motor.

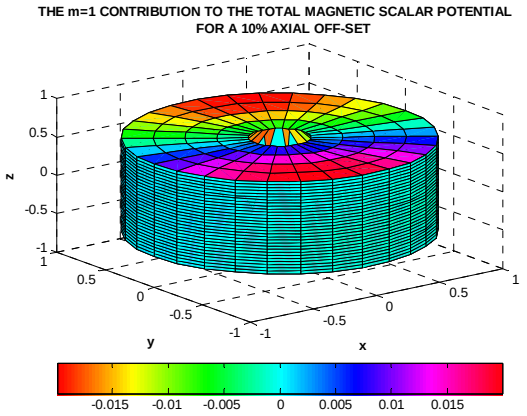

FIGURE 17 This is the $\Phi_P^{(1)}(\rho,\phi,z)$ component

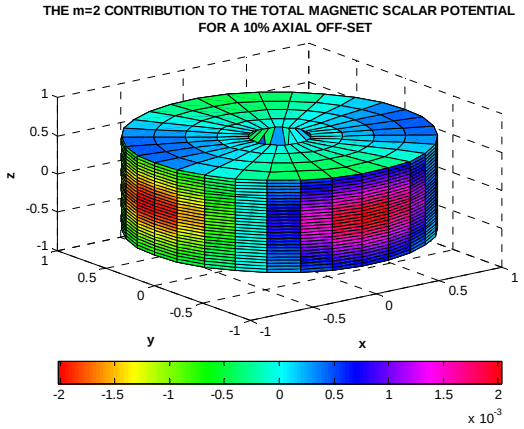

FIGURE 18 This is the $\Phi_P^{(2)}(\rho, \phi, z)$ component

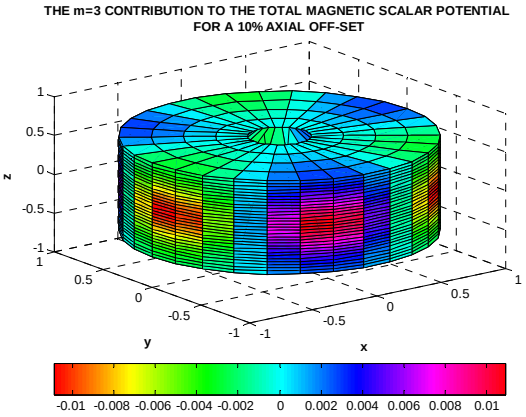

FIGURE 19 This is the $\Phi_P^{(3)}(\rho, \phi, z)$ component

One may notice that for the two unbalanced cases considered, a nontrivial dipole contribution appeared. This was not the case for the balanced motor. In fact, any sort of motor imbalance such as magnet demagnetization, axial or radial shifts, etc., will interrupt the symmetry of the balanced motor. This loss of symmetry will ultimately be reflected in the multipole distribution which describes the motor. This multipole description could be used to make predictions about the internal structure of the motor. In other words, by computing the multipole distribution of a real electrical machine, can one make predictions about what is causing the imbalance? This, of course, is a difficult question to answer with certainty. However, from the preliminary work done by the authors, it appears that one can make reasonable predictions, based upon anlaysis and experience, as to what causes specific motor imbalances and their corresponding multipole distributions. This would ultimately be a useful diagnostic tool.

DISCUSSION AND CONCLUSION

A general technique has been introduced for describing circular cylindrical magnetic systems. The Fourier series expansion or the toroidal expansion whose coefficients are the Q-functions can be used to represent a non-cylindrical magnetic source through the use of a method called charge simulation. The fictitious magnetic charges which are computed from charge simulation are located on a hypothetical cylinder which acts as the new magnetic source. Knowing the charge distribution on a cylinder greatly simplifies the mathematical problem since it allows one to immediately apply the magnetic form of Coulomb's law.

The main focus of this paper is to illustrate how the toroidal expansion can be employed to characterize, for example, a permanent-magnet motor in terms of its equivalent multipole distribution. It is shown that for a $6-pole$ balanced permanent magnet motor, the Q-function formulation predicts that the dominant term in the expansion is $m = 3$. Likewise, for a balanced $2n-pole$ permanent-magnet motor, the $m = \frac{Pole\ Number}{2} = n$ is the dominant contribution to the magnetic scalar potential or the magnetic field intensity. This is not the case when a motor has an imbalance. Under unbalanced conditions, things change. Other terms in the toroidal expansion contribute. This is to be expected, and one must, in general, consider various motor imbalances on a case-by-case basis for each type of motor that one chooses to study. However, for the permanent magnet motor that was studied in this paper, many test cases were performed and the authors have developed a tableau of various motor imbalances and their corresponding multipole distributions.

References

[1] Bouwkamp, C.J. and N.G. de Bruijn, "The Electrical Field of a Point Charge Inside a Cylinder, in Connection with Wave Guide Theory," Journal of Applied Physics, Vol. 18, pp. 562-577, 1947.

[2] Hobson, E.W., "On Green's Function for a Circular Disk, with applications to Electrostatic Problems", Transactions of the Cambridge Philosophical Society, Vol. 18, pp. 277-291, 1900.

[3] I.S. Gradshteyn, and I.M. Ryzhik, *Table of Integrals, Series, and Products*, Academic Press, 4^{th} ed., p.709, p. 732, 1980.

[4] Jackson, J.D., *Classical Electrodynamics*, John Wiley and Sons, 3^{rd} ed., pp. 117-119, 1999.

[5] Kwon, O-Mun, "The Analysis Of Effects Of Certain Asymmetries In Electrical Machines," Ph.D. dissertation, Rensselaer Polytechnic Institute, Troy NY, August 2003.

[6] Kwon, O-Mun, C.Surussavadee, M.V.K Chari, S.Salon, K.Sivasubramaniam, "Analysis of the Far Field Permanent Magnet Motors and study of effects of

geometric asymmetries and unbalance in magnet design," IEEE Transactions on Magnetics Vol. 40, No. 2, 435-442, 2004.

[7] Lebedev, N.N., *Special Functions and Their Applications*, Prentice-Hall, pp. 186-188, 1965.

[8] P.M. Morse, and H.Feshbach, *Methods of Theoretical Physics*, McGraw Hill, Parts I &II, p.744, pp.1301-1304, 1953.

[9] Schwab, A.J. *Field Theory Concepts*, Springer-Verlag, pp. 186-189, 1988.

[10] Selvaggi, J, "Multipole Analysis of Circular Cylindrical Magnetic Systems," Ph.D. dissertation, Rensselaer Polytechnic Institute, Troy NY, May 2005.

[11] Selvaggi, J., S. Salon, O-Mun Kwon, M.V.K Chari, "Calculating the External Magnetic Field from Permanent Magnets in Permanent-Magnet Motors-An Alternative Method," IEEE Transactions on Magnetics, Vol. 40, No. 5, pp. 3278-3285, September 2004.

[12] Smythe, W.R., *Static and Dynamic Electricity*, McGraw-Hill, 3^{rd} ed., p. 204, 1968.

[13] Snow, C., *Formulas for Computing Capacitance and Inductance,* National Bureau of Standards Circular 544, pp. 13-17, September 1, 1954.

[14] Snow, C., *Hypergeometric and Legendre Functions with Applications to Integral Equations of Potential Theory*, National Bureau Of Standards Applied Mathematics Series 19, U.S. Department of Commerce, pp. 228-252, May 1, 1952.

[15] Snow, C., *Potential Problems and Capacitance for a Conductor Bounded by Two Intersecting Spheres*, U.S. Department of Commerce NBS, Research Paper RP2032, Vol. 43, pp. 377-407, October 1949.

[16] Stratton, J. A, *Electromagnetic Theory*, McGraw-Hill Book Company, pp. 241-242, 1941.